ENHANCED PROTON ACCELERATION FROM A THIN TARGET IRRADIATED BY LASER PULSE**

M. Turki [1*], D. Bennaceur-Doumaz [2]

[1] *Radiation Physics Department, Faculty of Physics, University of Sciences and Technology Houari Boumediene (USTHB), Algeria; e-mail: mturki@usthb.dz*
[2] *Centre de Développement des Technologies Avancées (CDTA), Baba Hasse Algiers, Algeria*

The use of thin targets offers optimal conditions for accelerating protons to high energies from laser-matter interaction in the framework of the TNSA (target normal sheath acceleration) mechanism. Two-dimensional particle-in-cell (PIC) simulations were performed to investigate the effects of thickness and composition of targets in proton acceleration. We will demonstrate how proton energy increases with the target of a low atomic number Z by examining the energy spectra of the different materials He, C, and Al, whereby the maximum proton energy is obtained with a helium target.

Keywords: *proton acceleration, TNSA mechanism, PIC simulations, thin target, low Z material.*

УСКОРЕНИЕ ПРОТОНОВ С ТОНКОЙ МИШЕНИ ПРИ ОБЛУЧЕНИИ ЛАЗЕРНЫМ ИМПУЛЬСОМ

M. Turki [1*], D. Bennaceur-Doumaz [2]

УДК 621.375.826

[1] *Университет наук и технологий Хуари Бумедьен, Алжир; e-mail: mturki@usthb.dz*
[2] *Центр развития передовых технологий (CDTA), Баба Хассе, Алжир, Алжир*

(Поступила 19 октября 2022)

Использование тонких мишеней предлагает оптимальные условия для ускорения протонов до высоких энергий за счет взаимодействия лазера с веществом в рамках механизма TNSA. Двумерное моделирование частиц в ячейке (PIC) выполнено для исследования влияния толщины и состава мишеней на ускорение протонов. Показано, что энергия протонов увеличивается для мишени с низким атомным номером Z, проанализированы энергетические спектры He, C и Al. Максимальная энергия протонов достигается с гелиевой мишенью.

Ключевые слова: *ускорение протонов, механизм TNSA, PIC-моделирование, тонкая мишень, материал с низким Z.*

Introduction. Acceleration of charged particles by ultra-intense short laser pulses with high brightness, short duration, and low emittance has been widely explored in recent decades because of its prospective application in many areas, such as medical therapy [1], materials processing [2], charged particle radiography [3], and high energy density physics [4] and so on. To obtain high-quality and high-energy ion beams, different acceleration mechanisms are described. Among these mechanisms, the most widely investigated in proton acceleration is target normal sheath acceleration (TNSA) scheme [5]. The latter mechanism proceeds via the build-up of TV m^{-1} electrostatic fields at the rear side of a thin target foil, produced by hotter electrons generated at the laser-irradiated side of the target, typically via the oscillating $j \times B$ heating of linearly polarized light [6]. The energy spectrum of the accelerated protons could be controlled by appropriately choosing the laser and target parameters, such as laser energy, intensity, prepulse

** Full text is published in JAS V. 90, No. 5 (http://springer.com/journal/10812) and in electronic version of ZhPS V. 90, No. 5 (http://www.elibrary.ru/title_about.asp?id=7318; sales@elibrary.ru).

contrast, polarization, target thickness with its density and structure [7]. The use of ultrathin targets offers optimal conditions for accelerating protons to high energies from laser-matter interaction in the framework of the TNSA mechanism.

By performing two-dimensional particle-in-cell (PIC) simulations, we will demonstrate how the proton energy increased with low atomic number Z targets by examining the proton energy spectra of different materials by varying the target thickness.

PIC simulations set-up. PIC simulations are carried out using the open source code EPOCH (Extendable PIC Open Collaboration) [8] in which the core algorithm was developed by Dr. Chris Brandy and Dr. Keith Bennett at the University of Warwick (UK) [9] and based on an older code PSC (plasma simulation code) written by Hartmut Ruhl [10].

EPOCH is a plasma physics simulation that uses the PIC method [11] written in FORTRAN90. This method was extensively used to understand laser-driven ion acceleration mechanisms and to model ultra-high intensity, short-pulse laser experiments. A smaller number of pseudoparticles are used to represent the physical particles. The interface of EPOCH is straightforward as the user does not have to interact with the PIC code directly but instead defines parameters and initial conditions using an 'input deck'.

We assumed a simulation box of size $L_x \times L_y = 60 \times 20$ μm, from 0 to 60 μm in the x direction and between ±10 μm in the y direction. With square cells of 10 nm, it yields 6000×2000 cells in the simulation box. We introduced 48 electrons, 48 ions, and 100 protons by cell. We considered a laser pulse with a wavelength $\lambda_L = 0.8$ nm and a field amplitude $a_0 = eE_0/m_e\omega c = 7$ corresponding to an intensity $I = 1\times10^{20}$ W/cm^2. E_0 is the initial laser electric field amplitude, e is the electron charge, m_e is the electron mass, ω is the laser frequency, and c is the light speed. It has a pulse duration of 28 fs, and a spot size of 5 μm. The laser is linearly polarized and the boundaries are chosen as open in order to minimize the reflection effect. We considered a target with fully ionized atoms, of different materials, namely, He, C, and Al. A contaminant proton layer of 20 nm thickness is assumed on the backside of the target. The different material ions and electrons densities are given in Table 1.

TABLE 1. Volumetric Mass Density ρ, Ion Mass M, Ion density n_i, and Electron Density n_e of the Materials

Material	He	C	Al
Z	2	6	13
ρ, g/cm^3	0.178×10^{-3}	2	2.7
M, a. u.	4.00	12.01	26.98
n_i, 10^{22} cm^{-3}	2.68×10^{-3}	10.02	6.02
n_e, 10^{22} cm^{-3}	5.36×10^{-3}	60.12	78.26

Results and discussion. The effects of foil thickness and target composition on proton acceleration were studied using different materials (He, C, and Al) of varying thicknesses (50, 200, and 500 nm). We show in Fig. 1 the distribution of the electrostatic field in the longitudinal direction at 200 fs for a 50 nm thick target. The enhancement of the sheath field is clearly visible with a helium (Fig. 1a) target compared to that of carbon (Fig. 1b) and aluminum (Fig. 1c) targets, respectively. This is due to the increase of the electron density with helium.

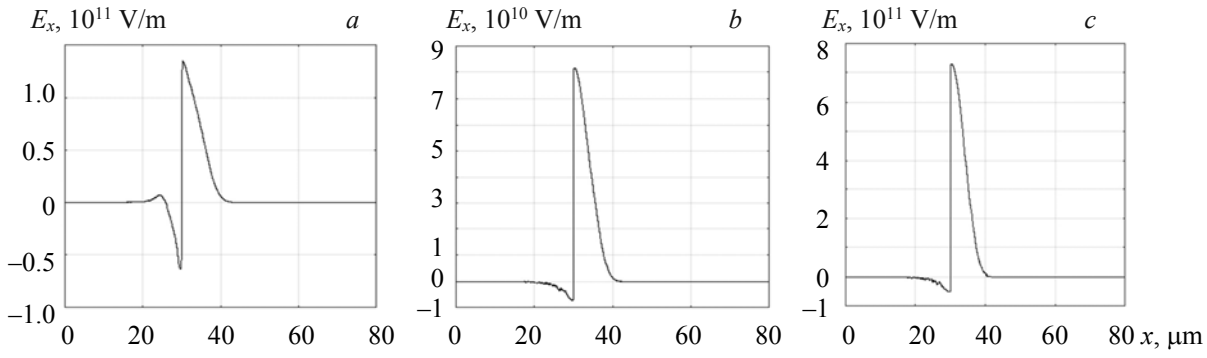

Fig. 1. Evolution of accelerating field along the longitudinal direction of propagation for different targets (a) helium, (b) carbon, (c) aluminum.

The proton energy spectra obtained for different foil thicknesses and compositions are plotted in Fig. 2. We observed a significant enhancement of maximum proton energy with the helium target, which is about a factor of 1.5 compared to the Al and C with a 50 nm thick target; this energy becomes smaller with thicker targets (200 and 500 nm).

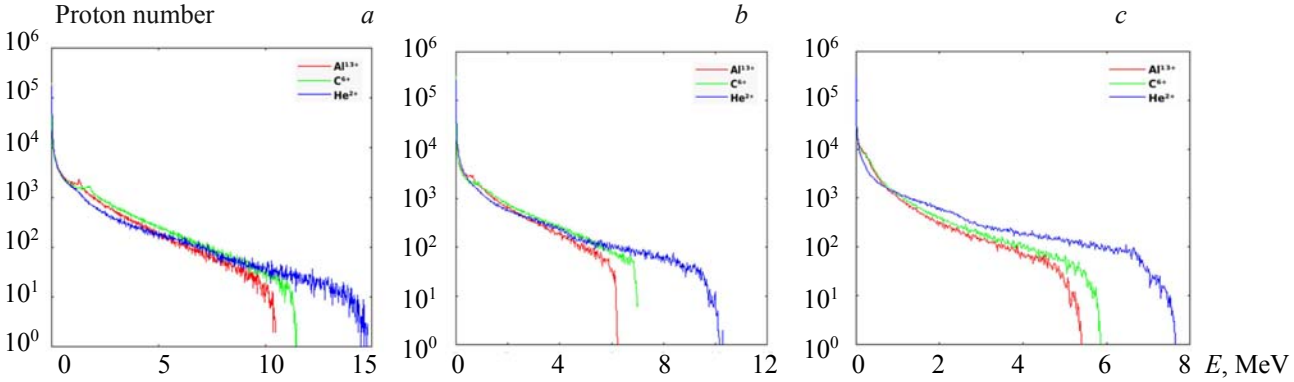

Fig. 2. The proton energy spectra from He, C, and Al for different target thicknesses (a) 50, (b) 200, and (c) 500 nm.

This can be understood as follows. The TNSA sheath electric field formed at the target rear surface created by the energetic electrons escaping from the rear surface is responsible for proton acceleration. These electrons are generated at the target front surface and propagate through the target with typical divergence angles [12]. The electric field is directly proportional to the square of the electron density as $E_{\mathrm{TNSA}} = \sqrt{(k_B T_e n_e)/\varepsilon_0}$ [13], where $k_B T_e$ is the electron temperature, n_e is the electron density at the rear target surface, and ε_0 is the permittivity in vacuum. The electron density itself is inversely proportional to the product of the target thickness and the tangent of the deviation angle of the electron beam crossing the target [14]. In addition, this angle is known to increase with the atomic number Z when the electrons are propagating through the target, undergoing several elastic collisions with the material ions [15]. Consequently, for thin targets and low Z, the density of hot electrons is increasing, which consequently results in the enhancement of the sheath field and hence the maximum proton energy.

In addition, the high-intensity interaction process is largely governed by the material mass, as a consequence, the helium ions are predicted to move $\sqrt{m_{Al}/m_{He}} = 2.59$ times and $\sqrt{m_{Al}/m_{He}} \approx 1.73$ times faster than aluminum and carbon. As a result, helium may decompose earlier (the fast electrons are produced earlier) than C and Al. This may explain the observed results in Fig. 3, when the proton energy is increasing with a low atomic number Z of the target. The maximum proton energy is then obtained with the helium target with the smallest thickness.

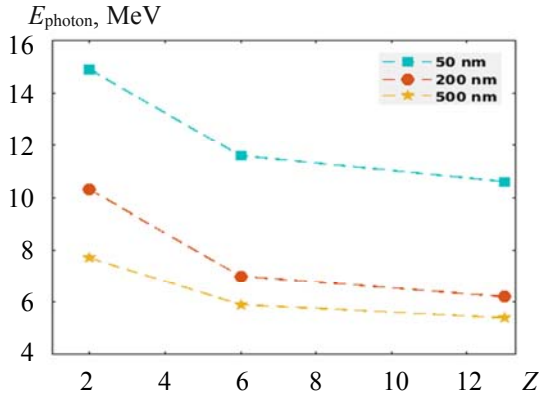

Fig. 3. The proton energy as a function of atomic number Z for different thicknesses.

Conclusions. It is found that materials of low Z are more favorable for enhancing proton energy with thin targets instead of commonly used elements (C, Al) usually used for proton acceleration in the TNSA mechanism.

REFERENCES

1. T. E. Cowan, U. Schramm, T. Burris-Mog, F. Fiedler, S. D. Kraft, K. Zeil, M. Baumann, M. Bussmann, W. Enghardt, K. Flippo, S. Gaillard, K. Harres, T. Herrmannsdoerfer, T. Kluge, F. Nürnberg, J. Pawelke, M. Roth, B. Schmidt, M. Sobiella, R. Sauerbrey, *AIP Conf. Proc*., **1299**, 721–726 (2010).
2. M. Stockman, *Phys. Today*, **64**, 39–44 (2011).
3. A. J. Mackinnon, P. K. Patel, R. P. Town, M. J. Edwards, T. Phillips, S. C. Lerner, D. W. Price, D. Hicks, M. H. Key, S. Hatchett, S. C. Wilks, *Rev. Sci. Instr*., **75**, 3531 (2004).
4. R. P. Drake1, P. Norreys, *New J. Phys*., **16**, 065007 (2014).
5. S. C. Wilks, A. B. Langdon, T. E. Cowan, M. Roth, M. Singh, S. Hatchett, M. H. Key, D. Pennington, A. MacKinnon, R. A. Snavely., *Plasma Phys*., **8**, 542–549 (2001).
6. G.-L. Jing, W. Yu, Y.-J. Li, S.-H. Zhao, L.-J. Qian, Y.-W. Tian, B.-C. Liu, *Acta Phys. Sin*., **55**, 3475–3479 (2006).
7. J. Badziak, *IOP Conf. Ser.: J. Phys.: Conf. Ser*., **959**, 012001 (2018).
8. T. D. Arber, K. Bennett, C. S. Brady, A. Lawrence-Douglas, M. G. Ramsay, N. J. Sircombe, P. Gillies, R. G. Evans, H. Schmitz, A. R. Bell, C. P. Ridgers, *Plasma Phys. Control. Fusion*, **57**, 113001 (2015).
9. K. Bennett, *EPOCH is the Extendable PIC Open Collaboration Project to Develop a UK Community Advanced Relativistic EM PIC Code*, https://cfsa-pmw.warwick.ac.uk/EPOCH/epoch.
10. H. Ruhl, *Classical Particle Simulations with the PSC code*, Academia.
11. W. L. Kruer, *The Physics of Laser Plasma Interactions*, California, Addison-Wesley Publishing Company (1988).
12. M. Tayyab, S. Bagchi, B. Ramakrishna, T. Mandal, A. Upadhyay, R. A. Ramis, J. Chakera, P. A. Naik, P. D. Gupta, *Phys. Rev. E*, **90**, 023103 (2014).
13. L. Torrisi, *Radiat. Eff. Defects Solids*, **171**, 34–44 (2016).
14. E. D. Tatomirescu, *Laser-Plasma Acceleration at Ultra-High Intensity Numerical Modeling*, PhD thesis, Bordeaux University, France (2019).
15. H. H. Hubbel, R. D. Birkhoff, *Phys. Rev. A*, **26**, 2460 (1982).